Journal of
Composites Science

MDPI

Article

Experimental Characterization of Fabric-Reinforced Cementitious Matrix (FRCM) Systems Applied on Calcarenite Stone: Adoption of Non-Standard Setup for Double-Shear Bond Tests

Maria Concetta Oddo [1,†], Liborio Cavaleri [1,*,†], Catherine Papanicolaou [2] and Lidia La Mendola [1]

[1] Department of Engineering, University of Palermo, 90128 Palermo, Italy; mariaconcetta.oddo01@unipa.it (M.C.O.); lidia.lamendola@unipa.it (L.L.M.)
[2] Department of Civil Engineering, University of Patras, 26504 Rio, Greece; kpapanic@upatras.gr
* Correspondence: liborio.cavaleri@unipa.it; Tel.: +39-09123896733
† These authors contributed equally to this work.

Abstract: The use of Fabric-Reinforced Cementitious Matrix (FRCM) systems is an innovative method for strengthening structures, particularly masonry, while addressing environmental and economic concerns. Despite their widespread use, characterizing FRCM composites poses challenges due to their complex mechanical behavior and considerable variability in properties. The available standardized testing methods exhibit some inconsistencies, underscoring the need for reliable characterization procedures. This paper presents an experimental study on the bond behavior between FRCM materials and calcarenite stone using a non-standard setup for double shear bond tests. Different FRCM systems are considered, varying the matrix composition and fabric nature. The experimental results are evaluated in terms of maximum stress, slip and data dispersion, alongside comparisons with double shear tests on larger samples and single-lap shear. These findings provide insights into how the mortar nature influences the stress-slip curves, strength, ductility and failure modes. The experimental study demonstrates the repeatability and robustness, particularly in terms of peak strength, of the non-standard setup configuration utilized in the study. The study highlights the importance of reliable characterization procedures for FRCM materials, especially in bond behavior assessments, emphasizing the need for further research to enhance our understanding of their application in structural reinforcement.

Keywords: FRCM; composites; masonry; strengthening systems; bond; mortar; glass fiber; basalt fiber

Citation: Oddo, M.C.; Cavaleri, L.; Papanicolaou, C.; La Mendola, L. Experimental Characterization of Fabric-Reinforced Cementitious Matrix (FRCM) Systems Applied on Calcarenite Stone: Adoption of Non-Standard Setup for Double-Shear Bond Tests. *J. Compos. Sci.* **2024**, *8*, 206. https://doi.org/10.3390/jcs8060206

Academic Editors: Yan Zhuge, Zhenhua Duan and Wahid Ferdous

Received: 4 April 2024
Revised: 21 May 2024
Accepted: 29 May 2024
Published: 31 May 2024

1. Introduction

The mechanical characterization of Fabric-Reinforced Cementitious Matrix (FRCM) composites for structural retrofitting applications has received noticeable interest from the technical and scientific community in the past few years. These composite materials, also known as Textile Reinforced Mortar (TRM) and Textile Reinforced Concrete (TRC) in the literature, have gained prominence due to their innovative use in numerous engineering applications. Their compatibility, reversibility, ease of installation, sustainability and vapor permeability make them particularly well-suited for application on masonry or stone substrates, as widely discussed in the literature [1–3].

FRCM composites, as commonly carried out in retrofitting applications of masonry structures, are placed in the tension zones of the structural members, aiming to carry enough tensile stress and increase the required structural performance, such as the in-plane shear and out-of-plane bending capacity [4,5] or giving a lateral confinement pressure to a column or pillar [6–8]. When loaded in tension, the mortar matrix of the FRCM composite is subjected to cracking, and the load is transferred to the textile, losing the compatibility of

the elongations between matrix and fiber [9,10]. Extensive research has been addressed to these bond conditions, particularly in the context of clay brick masonry [11,12], especially from an experimental point of view, with fewer investigations focused on natural stone supports [13].

In addition to exploring the physical and mechanical properties of FRCM constituents and their influence on bond performance [14–19], considerable attention within the scientific community has centered on the test methods used to characterize tensile and bond behavior.

This great interest was due to the need to draft Technical Standards and Guidelines concerning the mechanical characterization of FRCM composites. In recent times, Italian technical regulations were published to provide indications on test methods for the characterization and qualification of FRCM composites [20].

In the European framework, the regulations for performing shear bond tests are provided in the recommendations of RILEM TC 250-CSM [21]. The latter suggests characterizing the masonry-composite bond through single-lap tests. The sample consists of a prismatic substrate, as shown in Figure 1. To maximize the effective utilization of load transfer capacity from the FRCM system to the substrate, it is essential to apply the FRCM system on one side of the prismatic support, ensuring a bond width (B) ranging from 40 to 100 mm and a bond length (L) of at least 250 mm. These test methods need attention to detail. For example, ensuring the proper alignment of the fabric strip is crucial for achieving pure shear stress at the interface between the substrate and the matrix. Moreover, to promote a uniform distribution of stresses and prevent slippage, it is of fundamental importance to clamp the free end of the fiber strip securely to the testing machine using aluminum tabs.

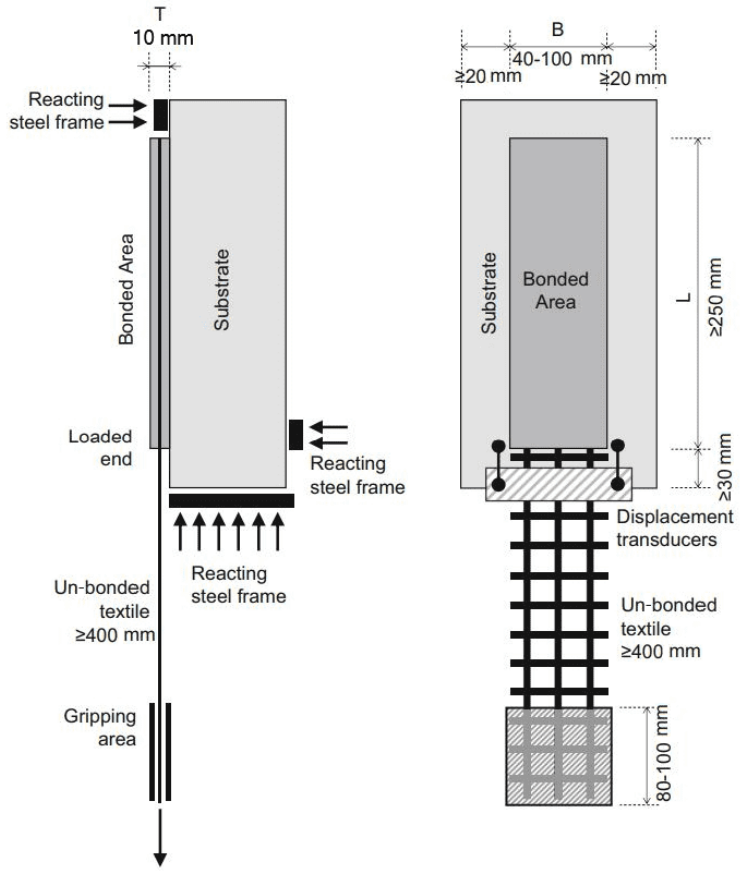

Figure 1. Suggested specimen geometry according to RILEM TC 250-CSM [21].

Before the publication of the RILEM recommendations, Ascione et al. [22] discussed the qualification methods of FRCM composites through the comparison of the results obtained from direct tensile tests and shear bond tests, defining the qualification limit

stress of the composite. This approach was later compared by De Santis et al. [23] with the approach of U.S. Standard AC434 [24,25], which proposes the use of tensile tests with a clevis-type gripping mechanism, instead of a combination of tests, for qualifying the tensile-bond behavior of the FRCM composite.

Carozzi et al. [26] compared the results of single and double direct shear bond test methods on polyparaphenylene benzobisoxazole (PBO), carbon and glass FRCM, proposing some details for each test. The influence of the testing apparatus, measuring devices, loading rate and clamping methods to be adopted in a RILEM-conforming test setup was more recently studied in a round-robin test program in Bellini et al. [27].

Despite the great amount of research work in this field, it is evident that further knowledge is needed, aiming to cover all the typologies of support and exploring possible alternative ways of testing. The different test methods available correspond to different drawbacks to be overcome: poor clamping pressure, stress concentration, non-uniform yarn slippage and premature failure [27–29].

This paper presents the characterization of the FRCM-to-calcarenite stone bond through a non-standard test setup for performing double-shear bond tests. Tests are performed on four types of FRCM, e.g., glass and basalt textile combined with a lime or cement-based mortar matrix. The setup is designed to have specimens with reduced weight and addresses the drawbacks associated with the already proposed single-lap shear bond test. These drawbacks include challenges in aligning the textile with the loading direction, avoiding stress concentration in the gripping area and compression stress on the support due to the contrasting steel frame system. The proposed configuration transforms the bond test into one that closely resembles a tensile test, drawing inspiration from the approach adopted by Accardi et al. [30] for studying the bonding behavior between FRP composites and masonry support.

In this experimental campaign, the support adopted is a natural calcarenite stone with a sedimentary origin. Calcarenite stone is a construction material commonly found in existing buildings of the Mediterranean area (specifically, Sicily), on which no previous bond tests with FRCM have been performed. In this sense, the current work aims to fill this gap in the literature, providing data about the compatibility of FRCM with this stone. Although the FRCM systems are generally applied to masonry structures, this study specifically investigates the bond performance on individual blocks of calcarenite stone. This choice reflects the characteristics of calcarenite masonry buildings, often characterized by thin mortar bed joints interposed with large unit blocks. Challenges and interactions introduced by these joints are beyond the scope of this work, but they represent a starting point for future investigation.

The experimental results are presented in terms of maximum strength deduced from FRCM-to-calcarenite bond tests and slip values, analyzing data dispersion to understand the consistency and reliability of the outcomes. Moreover, comparisons with double-shear tests on larger samples [31] and single-lap shear tests [32] allow for validation and verification of the experimental findings. These comparisons provide a broader context for interpreting the results and assessing the reliability of the bond testing methodology employed in the study.

2. Experimental Program

The experimental program involved the mechanical characterization of four composite systems, i.e., two basalt-based FRCM (BFRCM) and two glass-based FRCM (GFRCM) systems with two different mortar types, and their constituent materials. Double-Shear Bond (DSB) tests were performed, investigating the bond behavior of the FRCM systems applied on calcarenite support. In particular, three specimens were manufactured for each group by varying the fiber textile (i.e., basalt and glass grid) and the mortar type (i.e., cement and hydraulic lime-based mortar), as listed in Table 1.

Specimens were renamed according to the following designation XX_DSB_n, where XX indicates the fiber–mortar combination:

- BC is for BFRCM with cement-based mortar;
- BL is for BFRCM with hydraulic lime-based mortar;
- GC is for GFRCM with cement-based mortar;
- GL is for GFRCM with hydraulic lime-based mortar;
- DSB is for Double-Shear Bond test;
- n indicates the number of the specimen within each specimen group.

Table 1. Experimental program.

Specimen ID	Number of Specimens	Fiber Type	Mortar Type
BC_DSB_n	3	Basalt	Cement-based
BL_DSB_n	3	Basalt	Lime-based
GC_DSB_n	3	Glass	Cement-based
GL_DSB_n	3	Glass	Lime-based

2.1. Characterization of Constituent Materials

Calcarenite stone from the Sabucina quarry in Sicily (site of Italy) was adopted as masonry support for double-shear bond tests. This natural stone has a sedimentary origin and exhibits varying physical and mechanical characteristics depending on the extraction site. The calcarenite stone employed in this study exhibited the following mechanical properties, experimentally evaluated in a previous experimental campaign [33]: an average cube compressive strength of 14.7 MPa, a cylinder compressive strength of 12.9 MPa and an average elastic modulus in compression of 13,249 MPa.

In the current experimental campaign, two fibrous grids were employed as internal reinforcement of the FRCM systems: a coated bi-directional alkali-resistant basalt fiber grid with a mesh size of 6 × 6 mm, unit weight of 250 g/m^2 and equivalent thickness of 0.039 mm (Figure 2a) for the BFRCM systems and an alkali-resistant (AR) dry glass fiber grid with a mesh size of 12 × 12 mm, unit weight of 220 g/m^2 and equivalent thickness of 0.040 mm (Figure 2b) for the GFRCM systems. In order to verify the main mechanical characteristics, uniaxial tensile tests on nine coupons of basalt and glass fiber grid samples, oriented along the warp direction, were performed, according to UNI EN ISO 13934-1 standards [34]. In particular, tests were carried out under displacement control at a rate of 0.2 mm/min. Fiber coupons had dimensions of 50 mm in width, corresponding to eight and four yarns along the warp direction for basalt and glass textiles, respectively, and 400 mm in length. Moreover, aluminium tabs (50 × 75 mm) with a thickness of 2 mm were glued at the specimen extremities, using epoxy resin, to ensure the proper load distribution among the yarns in the gripping area.

Two bi-component pre-mixed mortars were adopted as matrices for the BFRCM and GFRCM systems. The former was a ready-mixed cement-based mortar with short glass fibers, pozzolanic aggregates, admixtures and synthetic polymers in water dispersion. The second was a lime-based mortar characterized by high ductility and hydraulic properties, composed of special additives and synthetic polymers dispersed in water. Flexural and compressive strength were experimentally evaluated by performing three-point bending tests and compressive tests on two batches (referred to as batch *a* and batch *b*) of each mortar type to assess the variability in the mechanical properties. A total of 24 mortar prisms were tested. In detail, 6 prisms (40 × 160 × 160 mm) were cast from each batch of mortar and tested to determine the flexural strength and, subsequently, the compressive strength was evaluated on 12 corresponding pieces. Both flexural and compressive tests were performed in displacement-control mode, assuming a rate of 0.5 mm/min, according to UNI EN 1015-11 standards [35].

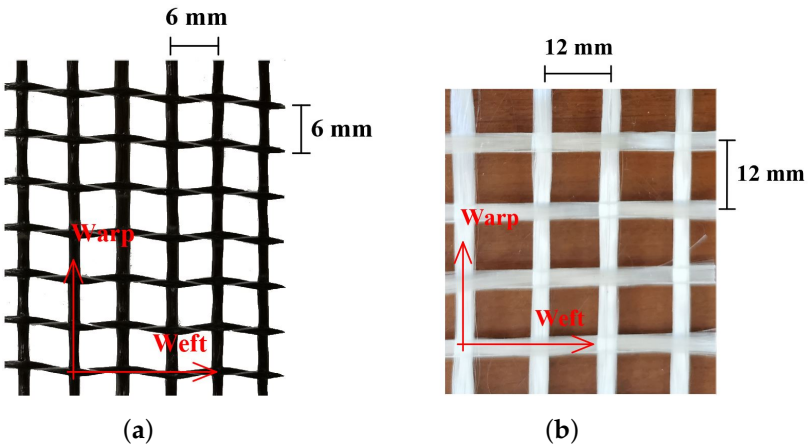

Figure 2. Fiber mesh: (**a**) Basalt; (**b**) Glass.

The mechanical performance of the four FRCM systems was evaluated by performing direct tensile tests on coupons with dimensions of 10 × 60 × 500 mm, following the recommendations of RILEM TC 232 TDT [36]. During the tests, the specimens' ends were clamped between two rigid steel plates, as shown in Figure 3. The gripping area spans a length of 125 mm and allowed for a degree of rotational capacity in the plane of the specimen.

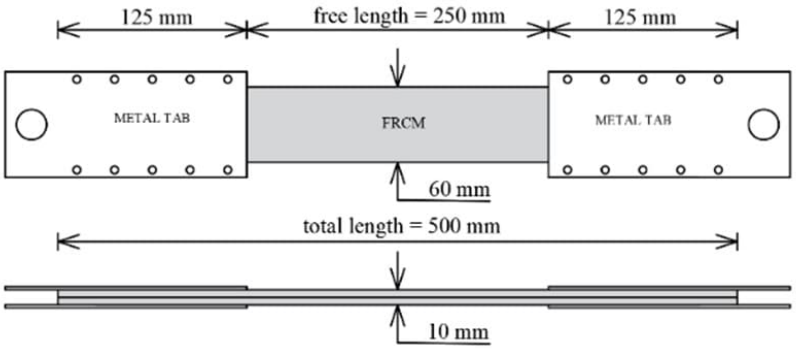

Figure 3. Geometry of composite coupons.

Each group of FRCM specimens was renamed with the following notations XX_TH, where XX indicates the fiber–mortar combination, in accordance with the designation used for specimens for bond tests (BC, BL, GC and GL) and TH stands for tensile test performed with clevis-grip method (T = Tensile test and H = Hinge grip). Coupons consisted of a single layer of basalt or glass textile placed such that the warp direction is parallel to the loading direction and embedded between two layers of mortar (cement- and lime-based) with an equal thickness of 5 mm. Moreover, a two-component adhesion promoter, water-based with low viscosity, was used to impregnate the glass grid to enhance the bond performance at the fiber–matrix interface for the GFRCM systems. It is worth pointing out that the adhesion promoter was not employed in the BFRCM systems as the basalt textile was already coated. Tensile tests were performed after 28 days of curing in controlled environmental conditions according to U.S. Standard AC434 [25]. Tests were carried out in displacement-control mode, with a rate of 0.2 mm/min, using a universal testing machine, as shown in Figure 4.

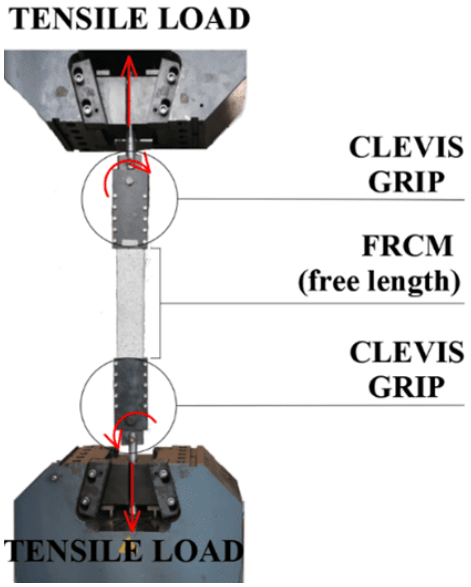

Figure 4. Setup for tensile test on composite coupons.

2.2. Specimens and Details for Double-Shear Bond Test Setup

Aiming to evaluate the bond performance of FRCM strengthening masonry supports, a novel application of a non-standard test setup for double-shear bond tests was proposed, as presented in Figure 5.

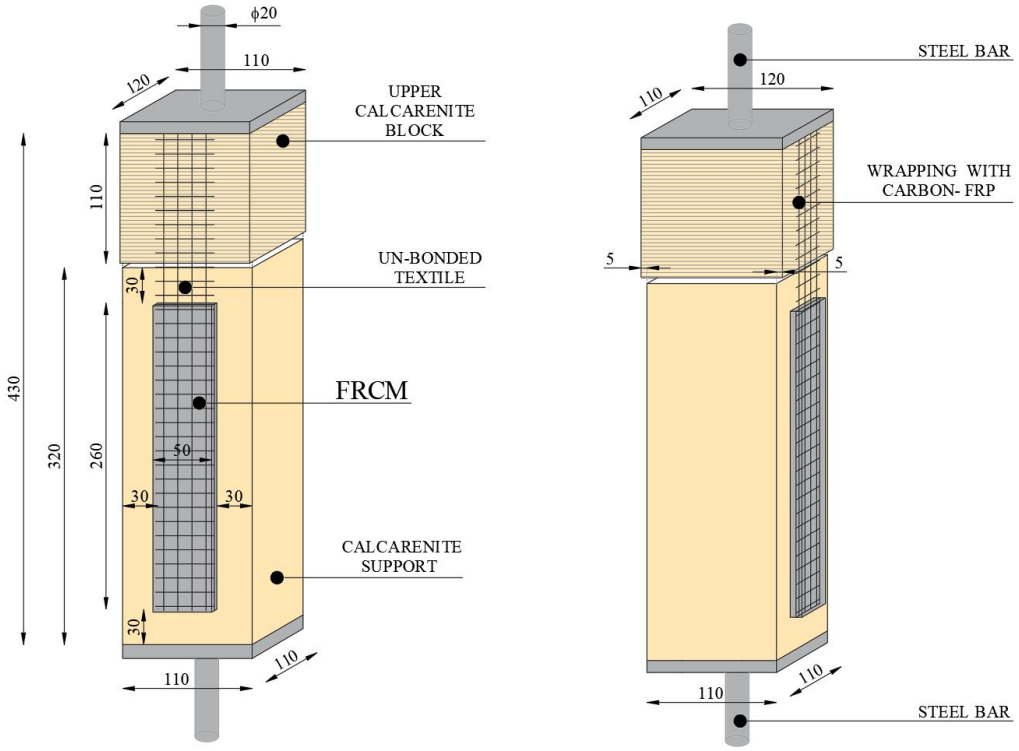

Figure 5. Geometry of specimen for shear bond test.

The tensile load was applied through the two steel bars by a universal testing machine, causing the direct shear on the two FRCM bonded strips, as shown in Figure 6. Tests were carried out in displacement-control mode, adopting a rate of 0.2 m/min up to failure. Two digital absolute displacement indicators were arranged on the two faces to measure the fibre-to-support slip close to the loading ends, as shown in Figure 7.

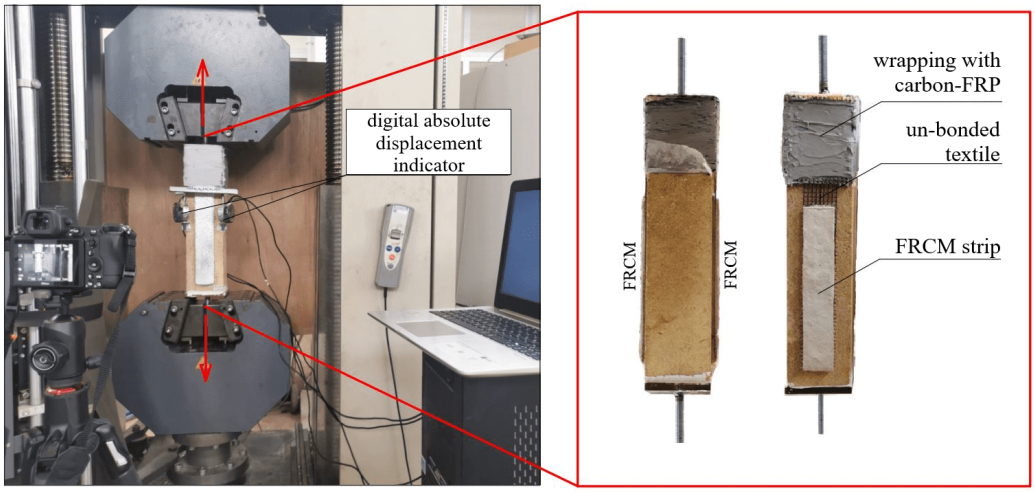

Figure 6. Non-standard, alternative test setup for double-shear bond test.

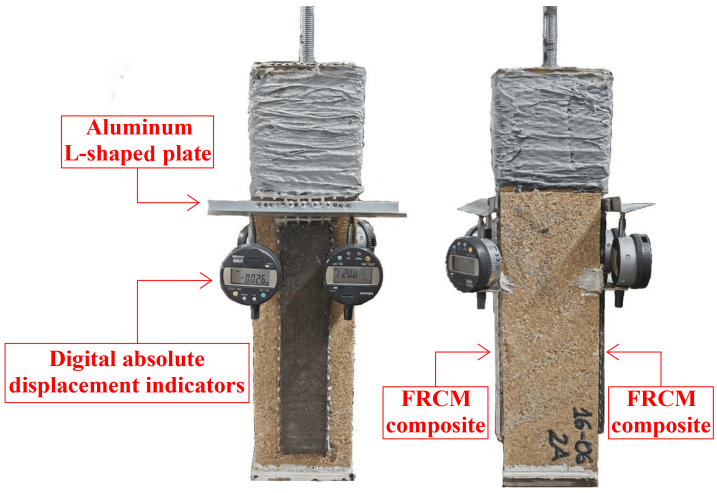

Figure 7. Arrangement of the digital absolute displacement indicators on a specimen.

3. Results from Material Characterization

Tensile tests on nine coupons of each fiber type provided the main mechanical properties. The average values and the Coefficient Of Variation (COV) of tensile strength and corresponding strain and elastic modulus are summarized in Table 2: tensile strength f_{fu} of 1142.2 MPa and 665.4 MPa and corresponding strains ε_{fu} of 1.61% and 1.09% and elastic moduli E_f of 71.8 GPa and 70.8 GPa for the basalt and glass fiber grids, respectively. Tensile strength values are calculated by dividing the maximum tensile load by the cross-sectional area of the textile A_f equal to 2.34 mm^2 and 2.40 mm^2 for the basalt and glass fiber grids, respectively. The strains are calculated for the gauge length adopted through the knife extensometers placed in the middle of the coupon, along a length of 80 mm.

Table 2. Average mechanical properties of basalt and glass fiber grids.

Fiber Grid	Average Tensile Strength f_{fu} [MPa]	Average Ultimate Strain ε_{fu} [%]	Average Elastic Modulus E_f [GPa]
Basalt	1142.2	1.61	71.8
COV	(14.3%)	(13.6%)	(5.7%)
Glass	665.4	1.09	70.8
COV	(10.2%)	(10.9%)	(9.7%)

The average results deduced from tests on six prisms of the two mortar matrices are summarized in Table 3. The flexural strength values of the two batches (*a* and *b*) of the cement-based mortar are quite close. However, the compressive strength of batch *a* is greater by 12.5% than the compressive strength of batch *b*. Conversely, the experimental compressive strengths of the lime-based mortar batches are quite similar. It should be noted that the observed high flexural strength of the lime-based mortar (6.6 MPa for batch *a* and 4.3 MPa for batch *b*) in light of the relatively low compressive strength can be attributed to the presence of short fibers within the pre-mixed mortar. These fibers, while not making a significant contribution to the compressive load-bearing capacity, play a crucial role in enhancing the flexural strength of the mortar. This enhancement arises from the capability of fibers to distribute the applied stresses more evenly, effectively mitigating the propagation of cracks.

Table 3. Average mechanical properties of the two mortar types: cement- and lime-based.

Mortar Type	Average Flexural Strength $f_{m,f}$ [MPa] (COV)	Average Compressive Strength $f_{m,c}$ [MPa] (COV)
Cement-based (batch *a*)	6.6 (6.1%)	40.7 (1.2%)
Cement-based (batch *b*)	6.2 (8.3%)	35.6 (6.1%)
Lime-based (batch *a*)	6.6 (6.1%)	16.2 (9.3%)
Lime-based (batch *b*)	4.3 (7.3%)	18.1 (0.8%)

The results from tensile tests on coupons of FRCMs are reported in terms of stress–strain curves in Figure 8. The stresses are calculated by dividing the recorded load values by the cross-sectional area of the bare textile (A_f), as suggested by Italian [20] and U.S. [25] guidelines. The strain values are obtained by considering the measurements of the knife sensors up to the end of the first linear elastic phase and the displacement measures of the machine cross-head in the post-elastic phase due to the unreliability of the knife sensors' measurements when crack opening occurs. These strain values are calculated by dividing the displacements measured by the knife sensors, positioned in the middle of the specimen, during the elastic phase by the gauge length of 80 mm and the displacement of the machine cross-head by the total specimen length in the post-cracking phase.

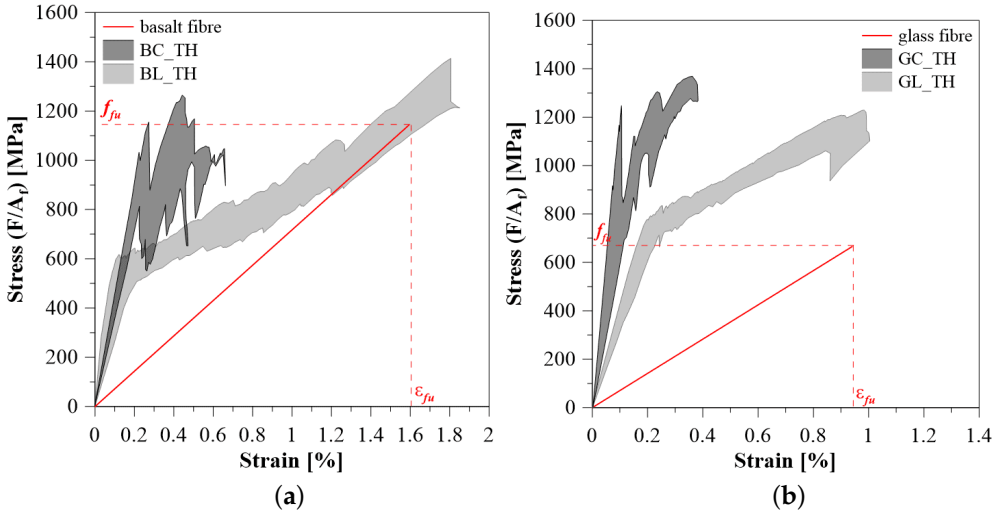

Figure 8. Stress–strain curves from tensile tests: (**a**) BFRCM systems with cement- and lime-based mortar (BC_TH and BL_TH); (**b**) GFRCM systems with cement- and lime-based mortar (GC_TH and GL_TH).

It is worth pointing out that the typical trend characterized by three response stages (as reported in Italian Guidelines [20]), was not always observed; these stages are the first

linear uncracked stage; the second stage of crack opening and development; and the third stage mainly governed by the fiber reinforcement and characterized by a slope similar to the elastic modulus of the bare fiber grid. The slope of the third stage was not recognizable for specimens of BFRCM (Figure 8a) and GFRCM (Figure 8b) with cement-based mortar (BC_TH and GC_TH). Therefore, the first cracking load is close to the tensile strength of the reinforcement layer, and the composite systems failed at lower values of strain.

This is due to the high strength of cement-based mortar resulting in an under-reinforced FRCM cross-sectional area. In this case, when the mortar failed in tension, the fiber mesh automatically failed as it cannot withstand the force carried by the mortar. Generally, a good adhesion was established at the fiber–mortar interface for samples of both BFRCM and GFRCM with cement-based mortar (BC_TH and GC_TH). Differently, sliding and debonding phenomena occurred between the basalt fiber grid and lime-based mortar (BL_TH). These phenomena were less evident in the case of GFRCM samples with lime-based mortar, possibly due to improved bond properties at the fiber–mortar interface resulting from the use of the adhesion promoter. With lime-based mortar, cracking was observed, and the fiber textile withstood higher loads than its tensile strength alone. This is probably due to the textile being primed with bond-enhancing agents. These agents infiltrate the fiber yarns and bond the individual filaments together, thus alleviating the intra-yarn differential stretching of the filaments. Additionally, the stress distribution among the glass fiber yarns is more uniform in the composite strips because of the greater mortar contribution than with the coupons of the dry glass grid.

The main average results from direct tensile tests on nine coupons for each of the four FRCM systems are summarized in Table 4: the average first crack stress, the average peak stress and corresponding peak strain and the average slope of the third branch of the tensile curve, if recognizable. Additionally, the exploitation ratio of the fiber reinforcement is reported. The latter is calculated by dividing the maximum tensile strength of the composite by the tensile strength of the fiber textile. In particular, the exploitation ratio of fiber for the BFRCM samples is close to 1, i.e., 1.02 and 1.11 for BC_TH and BL_TH, respectively. While the exploitation ratios of fiber for the GFRCM samples highlight that the samples attain a maximum tensile strength that is about 91% and 70% larger than the tensile strength of the glass fiber grid.

Table 4. Average results of FRCM composites tested in tension.

FRCM System	First Crack Stress [MPa]	Peak Stress [MPa]	Strain at Peak Stress [%]	Slope of Third Stage [GPa]	Exploitation Ratio of Fiber [-]
BC_TH	995.4	1161.6	0.36	nd	1.02
BL_TH	562.5	1268.9	1.69	69.0	1.11
GC_TH	1100.2	1271.8	0.29	nd	1.91
GL_TH	695.9	1127.9	0.85	63.0	1.70

nd = data not available.

4. Double-Shear Bond Experimental Tests: Main Results

4.1. Stresses and Corresponding Displacements

The outcomes of the tests on the objects are reported in Figure 9. The curves inserted in this figure correlate stresses and displacements, being the stresses obtained as a ratio between the tensile force and the nominal cross-section area of the fiber grid A_f (equal to 1.95 mm^2 and 2.00 mm^2 for basalt and glass fiber, respectively). The displacement is that of the calcarenite block at the head of each specimen due to the slip of the fiber layer in the support and the deformation of the fiber strip non-bonded.

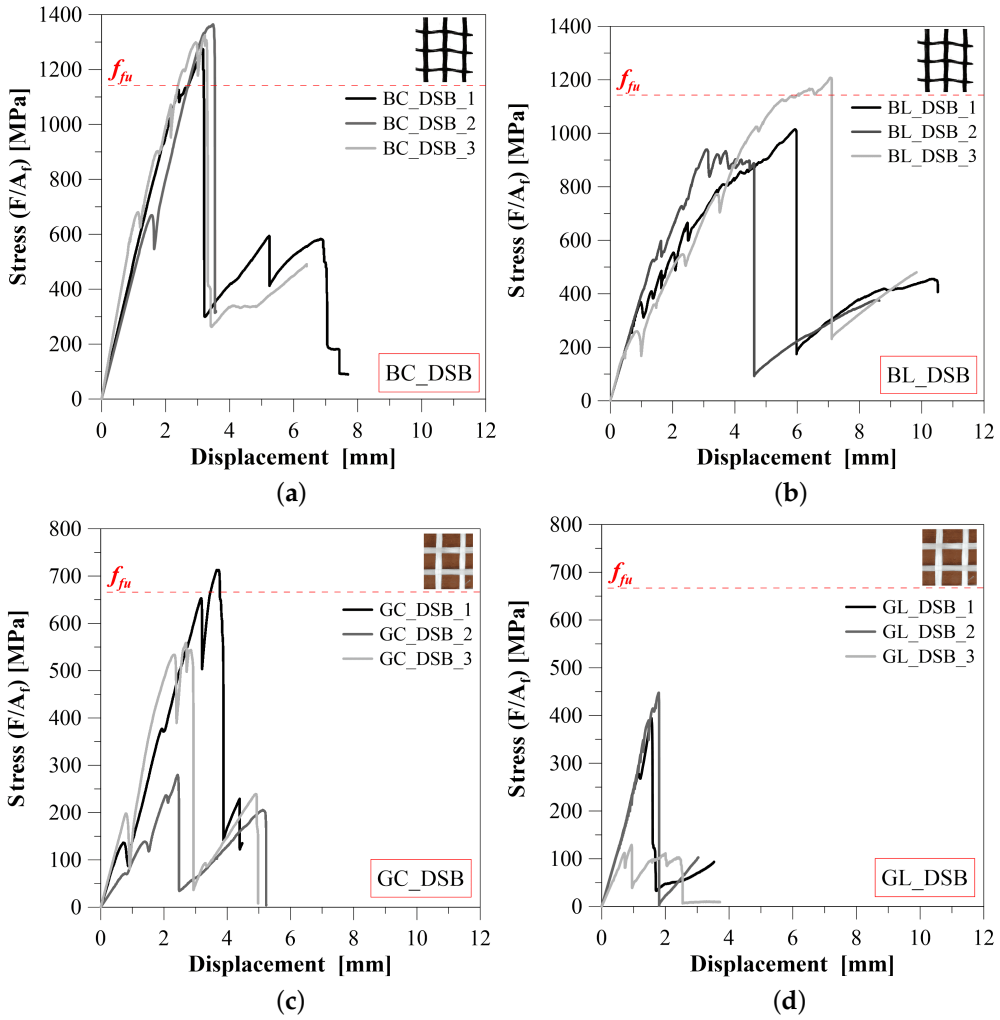

Figure 9. Stress–displacement curves from double-shear bond tests: (**a**) BFRCM with cement-based mortar (BC_DSB); (**b**) BFRCM with lime-based mortar (BL_DSB); (**c**) GFRCM with cement-based mortar (GC_DSB); (**d**) GFRCM with lime-based mortar (GL_DSB).

Generally, the curves comprise an initial linear branch that rapidly becomes nonlinear. Then, the failure of the grid, causing a sudden reduction of the load and consequently of the nominal stress, is observed (Figure 9a,c,d), or the detachment at the fiber-top mortar layer interface (Figure 9b). Moreover, a residual capacity is observed due to the undamaged yarns (for samples of groups: BC_DSB, GC_DSB and GL_DSB) or the residual stress at the textile–matrix interface due to friction (for samples of group BL_DSB).

The experimental results are reported in Table 5. In detail, the peak strength, the displacement at the peak strength and the failure mode are reported (averages and Coefficient of Variation are also included). For the failure modes, the notation recommended by the RILEM Technical Committee 250-CSM recommendations [21] has been used, as reported in Table 6.

Moreover, the exploitation ratios versus the bare textile and versus the corresponding FRCM composite system are reported. These ratios are determined by dividing the peak stress achieved during double-shear bond tests by the respective average experimental tensile strength of the bare textile and the average peak stress observed during tensile tests on FRCM composite specimens.

Table 5. Results from double-shear bond tests on BFRCM and GFRCM used as reinforcement of calcarenite blocks.

Sample ID	Peak Strength [MPa]	Disp. at Peak Strength [mm]	Exploitation Ratio vs. Fibre [-]	Exploitation Ratio vs. Composite [-]	Failure Mode
BC_DSB_1	1274.3	3.17	1.12	1.10	E2
BC_DSB_2	1364.3	3.48	1.19	1.17	E1
BC_DSB_3	1324.5	3.23	1.16	1.14	E1
Average	1321.0	3.29	1.16	1.14	
COV	(2.8%)	(4.1%)	(2.8%)	(2.8%)	
BL_DSB_1	1015.0	5.94	0.89	0.80	D/C
BL_DSB_2	939.6	3.11	0.82	0.74	C/A
BL_DSB_3	1207.7	7.06	1.06	0.95	C/A
Average	1054.1	5.37	0.92	0.83	
COV	(10.7%)	(31.0%)	(10.7%)	(10.7%)	
GC_DSB_1	712.9	3.67	1.07	0.56	E1
GC_DSB_2	279.6 *	2.43 *	0.42 *	0.22 *	E1
GC_DSB_3	558.8	2.69	0.84	0.44	E1
Average	635.9	3.18	0.96	0.50	
COV	(12.1%)	(15.3%)	(12.1%)	(12.1%)	
GL_DSB_1	394.6	1.17	0.59	0.35	E1
GL_DSB_2	447.8	1.79	0.67	0.40	E1
GL_DSB_3	129.0	0.94	0.19	0.11	E1
Average	323.8	1.30	0.49	0.29	
COV	(43.1%)	(27.8%)	(43.1%)	(43.1%)	

* Result discarded from the calculus of the mean.

Table 6. Notation for the failure mode based on RILEM Technical Committee 250-CSM Recommendations [21].

Symbol for Failure Mode	Description
A	Cohesive debonding of the cementitious matrix at the contact layer with calcarenite stone
C	Debonding of the fabric fibers
D	Textile slippage in the cementitious matrix
E1	Rupture of the textile out of the cementitious matrix
E2	Rupture of the textile in the matrix

The COV values listed in Table 5 provide a measure of the scattering of the results. In detail, the results (excluding those of the GL_DSB group) are quite uniform in terms of peak strength, while higher differences are observed in terms of displacement when sliding (failure mode D) and debonding phenomena occur at the interface level (failure mode A or C), e.g., in the case of the BL_DSB specimens (COV value is equal to 31.0%).

The test uncertainties were much higher when bond tests on specimens of group GL_DSB were performed. In this case, the COV reached 43.1% for peak strength and 27.8% for the corresponding slip. This difference in the uncertainty was likely due to an accidental loading eccentricity for imperfections in the manufacturing of the specimens. This fact caused a non-uniform transfer of the load to the two bare fiber strips. This issue was not noticed in specimens with basalt fibers since the bare textile is rigid and can easily be positioned correctly. A difference in the load transferred to the glass fiber strips was revealed by the measurement of the fiber-to-support slip by the transducers located as shown in Figure 7. The load–slip and load–displacement correlations are shown in Figure 10.

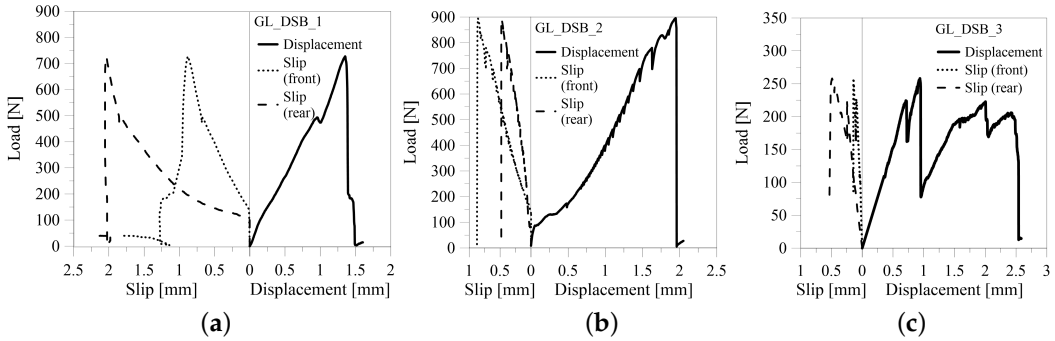

Figure 10. Load–slip and load–displacement correlations for GL_DSB specimens: (**a**) GL_DSB_1; (**b**) GL_DSB_2; (**c**) GL_DSB_3.

4.2. Failure Modes

Cement-based mortar specimens, i.e., group BC_DSB and GC_DSB, exhibited tensile failure of the textile (failure mode E1 or E2). Generally, the fiber rupture occurred out of the matrix in the free un-bonded length (failure mode E1) as shown in Figure 11a,b for specimen BC_DSB_1 and GC_DSB_2, respectively.

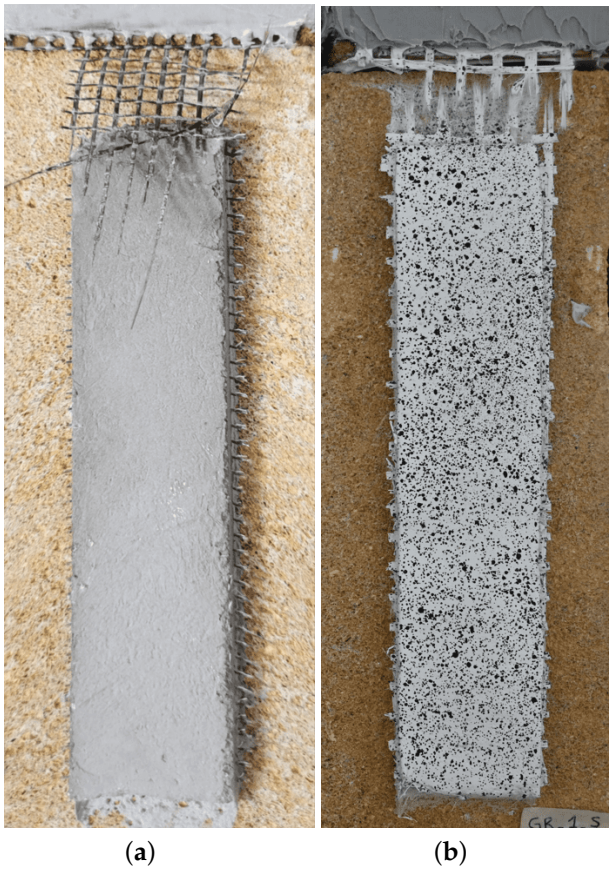

Figure 11. Failure of textile (E1): (**a**) specimen BC_DSB_1; (**b**) specimen GC_DSB_2.

BFRCM specimens with lime-based mortar (i.e., group BL_DSB) exhibited the detachment of the external layer of mortar, which debonded from the textile (failure mode C). Furthermore, fiber sliding (failure mode D) occurred in specimen BL_DSB_1, as shown in Figure 12a. When the external layer of mortar entirely detached (Figure 12b), the experiment was ended. For samples BL_DSB_2 and BL_DSB_3, failure mode C (debonding at the fiber–matrix interface) over an average length of 85 mm was observed. Then, cohesive debonding occurred (failure mode A—Figure 12c).

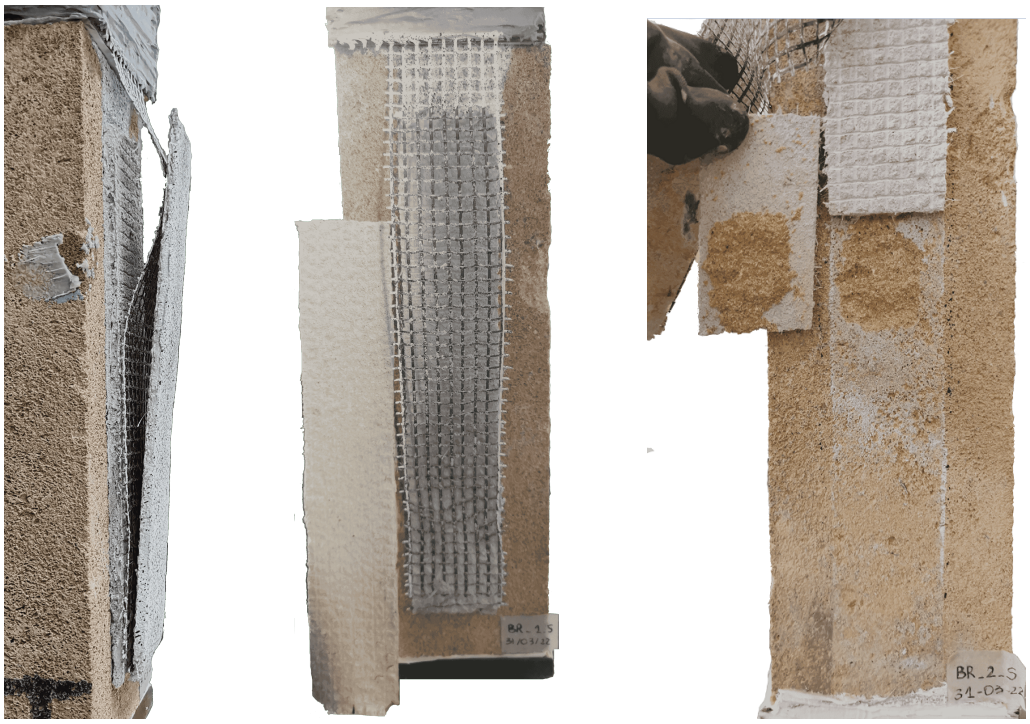

(**a**) (**b**) (**c**)

Figure 12. Failure mode for specimens of group BL_DSB: (**a**) debonding at fiber–matrix interface; (**b**) total detachment of the upper mortar layer; (**c**) cohesive debonding in the substrate.

The samples of group GL_DSB failed due to the premature tensile rupture of the un-bonded glass grid without debonding at the mortar–textile interface, sliding, or cracks formation in the mortar layer. This was caused by a stress concentration in a single un-bonded fiber strip for the eccentric loading as discussed above.

5. Comparisons and Discussion

The results, obtained from the double-shear bond test using the proposed non-standard test setup, have been compared to the results obtained from double-shear tests conducted on larger samples, available in [31], and single-lap shear tests available in [32]. These results, derived from bond tests carried out on samples characterized by the same BFRCM systems, with mortar made with cement and lime and with calcarenite stones with the same origin as that used in the present experimental campaign, provide insights on scale effects (for the same type of shear bond test) and the differences connected to the execution of not-equal shear bond tests.

The comparisons of stress–displacement curves for BFRCM strips bonded on calcarenite masonry substrate with the available results referred to double-lap shear bond tests on larger samples are plotted in Figure 13. These comparisons allow us to investigate the influence of FRCM bond length and width. Specifically, the results obtained from the current experimental campaign pertain to an FRCM bond length of 260 mm and a bond width of 50 mm. These findings are compared with those from samples of larger dimensions, featuring a bond length of 320 mm and a width of 100 mm for the BFRCM strip [31].

It is noteworthy that the slopes of the curves from the double-shear bond tests conducted on both small (using the proposed setup configuration) and larger samples (as reported in the literature) are quite similar for BFRCM specimens with cement-based (Figure 13a) and those with lime-based mortar (Figure 13b) during the initial ascending branch.

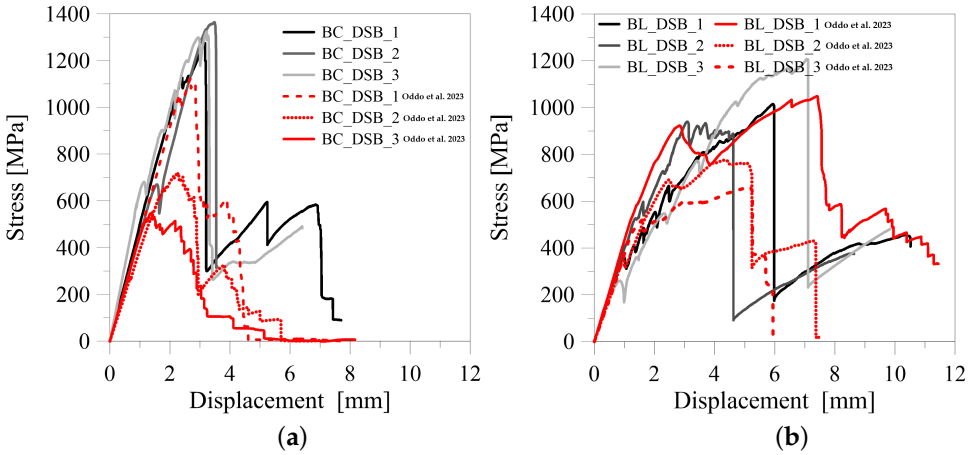

Figure 13. Comparisons with available results referred to double-lap shear bond tests on larger samples from Oddo et al. [31]: (**a**) BFRCM with cement-based mortar; (**b**) BFRCM with lime-based mortar.

However, some inconsistencies between the results are observed. Notably, a large scatter is observed in the bond tests performed on larger samples of BFRCM with cement-based mortar (BC) (Figure 13a). Only specimen BC_DSB_1 of Ref. [31] exhibits a trend (dashed red curve) similar to the curves obtained from specimens tested with the proposed test setup configuration. This scatter is probably attributable to the influence of the test setup configuration, as also observed in numerous studies available in the literature [18,28]. The eccentricity resulting from variations in composite size is likely the primary cause of the scatter in peak stress. This is because ensuring a uniform load distribution among a larger number of longitudinal yarns becomes more challenging, compounded by the potential presence of additional defects on a wider un-bonded fiber strip.

Additional differences are observed when fiber slippage and debonding at the fiber–mortar interface occur (Figure 13b). The specimens of BFRCM with a lime-based mortar tested on small and larger samples [31] exhibit approximately the same initial stiffness in the first almost linear branch, followed by a nonlinear phase characterized by significant scatter. This behavior is attributed to the heightened complexity of the fiber–mortar interaction [37,38].

The average stress–displacement curves comparing BFRCM strips bonded onto calcarenite stone with available results from single-lap shear bond tests and double-shear bond tests on larger samples are reported in Figure 14. These comparisons allow us to investigate the differences of the double-shear bond test setup compared to the single-lap shear bond test setup [32].

In contrast to previous comparisons, the curves representing single-lap shear bond tests on BFRCM with cement-based mortar (Figure 14a) exhibited lower stiffness compared to the curves obtained from the proposed double-shear bond test. Further, peak stress values obtained from single-lap shear bond tests are significantly scattered, as for the corresponding ultimate displacement values. This variability is likely attributed to the challenge of ensuring proper alignment of the un-bonded fiber strips with respect to the composite, which can be more complex [39]. The occurrence of accidental load eccentricity is fundamental since it can significantly compromise the results. When the tensile load applied on the fiber is eccentric, it is not transferred as pure shear stress onto the composite because stress in the orthogonal direction occurs at the fiber–mortar interface. The occurrence of stress in the orthogonal direction leads to the detachment of the upper mortar interface layer, compromising the results [40].

The curve referred to the single-lap shear test on BFRCM with lime-based mortar (Figure 14b) shows a peak strength quite close to the average peak strength derived from double-shear bond tests, although a different stiffness was obtained from single-lap shear bond test. Further, the first phase with a lower slope is due to inadequate adjustment of the

sample at the beginning of the test. However, only one test provided in Bramato et al. [32] for BFRCM with lime-based mortar is not significant for the repeatability of the results.

In general, the scatter in the results according to the proposed test setup was lower in connection to the strategy of the transfer of loads to the FRCM strips, as well as for setups adopted in [31,32]. Moreover, these results align with the performance and the failure modes observed in tensile tests on the corresponding FRCM coupons: i.e., tensile failure of fiber for BFRCM with cement-based mortar and debonding at the fiber–mortar interface for BFRCM with lime-based mortar.

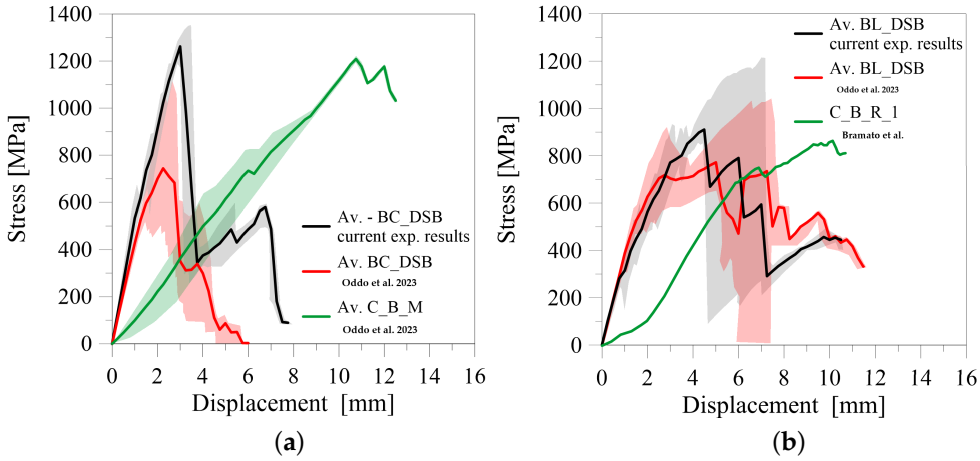

Figure 14. Comparisons of average curves from the current experimental campaign, double-lap shear bond tests on larger samples from Oddo et al. [31], and single-lap shear bond tests from Bramato et al. [32]: (**a**) BFRCM with cement-based mortar; (**b**) BFRCM with lime-based mortar.

6. Conclusions

This paper presented the results of an experimental investigation on the bond behavior of different FRCM systems for the reinforcement of calcarenite stones (or masonry), proposing an application of a non-standard test setup. Different types of FRCM are considered: with glass or basalt fiber grid; with cement- or lime-based mortar. The role of the involved materials is investigated.

Based on the results obtained and the range of variables analyzed, the following conclusions can be drawn:

- The type of mortar significantly affects bond properties at the fiber–mortar interface and thus, the behavior of FRCM systems. Coated basalt textiles exhibit limited adhesion with lime-based mortar, while glass textiles demonstrate good adhesion with lime-based mortar, and both glass and coated basalt textiles exhibit strong adhesion with cement-based mortar. The lime-based BFRCM facilitated gradual energy dissipation over abrupt failure modes, thereby avoiding the sudden energy release associated with fiber rupture and allowing for the energy-consuming mechanism of gradual fiber slippage.
- Experimental results show a minimal influence of the calcarenite support, primarily evident when significant interface mechanisms develop at the fiber–matrix level.
- Double-shear bond tests, with a non-standard setup configuration, proved to be repeatable and reproducible, especially in terms of peak strength. Low scatter is observed, except in cases such as specimens of GFRCM with lime-based mortar where manufacturing-related issues arise due to the sensitivity of dry fiber textiles to alignment problems. This sensitivity prevents the reinforcement system from effectively redistributing loads when the most stressed fiber yarns fail.
- The number of specimens tested herein is admittedly limited and more specimens should be tested to statistically validate the results; additionally, there is a size-dependent scattering effect (also present in other shear bond test configurations) that needs to be further investigated.

Based on the discussed results it is not wrong to state that the behavior (strength and failure mode) is strongly connected with the fiber characteristics and the fiber–mortar interaction, the type of matrix and the manufacturing accuracy of samples, while the calcarenite stone demonstrated to be a strong support for the application of the external FRCM system. Although this result supports the application of FRCM for retrofitting applications on masonry structures made with calcarenite stone units, further investigations are desirable to confirm these conclusions.

Author Contributions: Conceptualization, M.C.O., L.C. and L.L.M.; methodology, M.C.O., L.C. and L.L.M.; validation, M.C.O., L.C. and L.L.M.; formal analysis, M.C.O., L.C. and L.L.M.; investigation, M.C.O. and L.L.M.; data curation, M.C.O.; writing—original draft preparation, M.C.O.; writing—review and editing, L.C., C.P. and L.L.M.; visualization, L.C. and L.L.M.; supervision, L.C., C.P. and L.L.M.; project administration, L.L.M.; funding acquisition, L.L.M. All authors have read and agreed to the published version of the manuscript.

Funding: This research was carried out within the RETURN Extended Partnership and received funding from the European Union Next-Generation EU (National Recovery and Resilience Plan–NRRP, Mission 4, Component 2, Investment 1.3–D.D. 1243 2/8/2022, PE0000005).

Data Availability Statement: The original contributions presented in the study are included in the article.

Conflicts of Interest: The authors declare no conflicts of interest.

References

1. Cucuzza, R.; Domaneschi, M.; Camata, G.; Marano, G.C.; Formisano, A.; Brigante, D. FRCM retrofitting techniques for masonry walls: A literature review and some laboratory tests. *Procedia Struct. Integr.* **2023**, *44*, 2190–2197. [CrossRef]
2. Yuan, Y.; Milani, G. Double shooting method for FRCM reinforced systems in debonding problems. *Compos. Struct.* **2024**, *339*, 118136. [CrossRef]
3. Lignola, G.P.; Manfredi, G.; Prota, A. Effects of Defects on Masonry Confinement with Inorganic Matrix Composites. *Materials* **2023**, *16*, 4737. [CrossRef] [PubMed]
4. Del Zoppo, M.; Di Ludovico, M.; Balsamo, A.; Prota, A. Fibre reinforced mortars for the out-of-plane strengthening of masonry walls. *Procedia Struct. Integr.* **2023**, *44*, 2158–2165. [CrossRef]
5. D'Antino, T.; Bertolli, V.; Cagnoni, A.; Calabrese, A.S.; Poggi, C. Bending and shear behavior of historic walls strengthened with composite reinforced mortar. In Proceedings of the 11th International Conference on Fiber-Reinforced Polymer (FRP) Composites in Civil Engineering (CICE 2023), Rio de Janeiro, Brazil, 23–26 July 2023 ; Harries, K., Cardoso, D.C.T., Silva, F.A., Eds.; pp. 1–10.
6. Maddaloni, G.; Cascardi, A.; Balsamo, A.; Di Ludovico, M.; Micelli, F.; Aiello, M.A.; Prota, A. Confinement of full-scale masonry columns with FRCM systems. *Key Eng. Mater.* **2017**, *747*, 374–381. [CrossRef]
7. Aiello, M.A.; Cascardi, A.; Ombres, L.; Verre, S. Confinement of masonry columns with the FRCM-system: Theoretical and experimental investigation. *Infrastructures* **2020**, *5*, 101. [CrossRef]
8. Di Ludovico, M.; Cascardi, A.; Balsamo, A.; Aiello, M.A. Uniaxial experimental tests on full-scale limestone masonry columns confined with glass and basalt FRCM systems. *J. Compos. Constr.* **2020**, *24*, 04020050. [CrossRef]
9. Saidi, M.; Gabor, A. Use of distributed optical fibre as a strain sensor in textile reinforced cementitious matrix composites. *Measurement* **2019**, *140*, 323–333. [CrossRef]
10. Grande, E.; Milani, G.; Imbimbo, M. Theoretical model for the study of the tensile behavior of FRCM reinforcements. *Constr. Build. Mater.* **2020**, *236*, 117617. [CrossRef]
11. Reboul, N.; Saidi, M.; Mualla, S.; Homoro, O.; Amziane, S. Bond behaviour of Fibre Reinforced Polymers applied on masonry substrate: Analysis based on acoustic emission, digital image correlation and analytical modelling. *Constr. Build. Mater.* **2023**, *403*, 132921. [CrossRef]
12. Rotunno, T.; Fagone, M.; Grande, E.; Milani, G. FRCM-to-masonry bonding behaviour in the case of curved surfaces: Experimental investigation. *Compos. Struct.* **2023**, *313*, 116913. [CrossRef]
13. Bramato, G.; Leone, M.; Ceroni, F.; Oddo, M.C.; Minafò, G.; Aiello, M.A.; La Mendola, L. State of the art on bond between frcm systems and masonry/concrete substrate: Database analysis and improved models. *Procedia Struct. Integr.* **2023**, *44*, 2310–2317. [CrossRef]
14. D'Ambrisi, A.; Feo, L.; Focacci, F. Experimental analysis on bond between PBO-FRCM strengthening materials and concrete. *Compos. Part B Eng.* **2013**, *44*, 524–532. [CrossRef]
15. Sneed, L.; D'Antino, T.; Carloni, C.; Pellegrino, C. A comparison of the bond behavior of PBO-FRCM composites determined by double-lap and single-lap shear tests. *Cem. Concr. Compos.* **2015**, *64*, 37–48. [CrossRef]
16. Olivito, R.S.; Codispoti, R.; Cevallos, O.A. Bond behavior of Flax-FRCM and PBO-FRCM composites applied on clay bricks: Experimental and theoretical study. *Compos. Struct.* **2016**, *146*, 221–231. [CrossRef]

17. Bilotta, A.; Ceroni, F.; Nigro, E.; Pecce, M. Experimental tests on FRCM strengthening systems for tuff masonry elements. *Constr. Build. Mater.* **2017**, *138*, 114–133. [CrossRef]
18. Leone, M.; Aiello, M.A.; Balsamo, A.; Carozzi, F.G.; Ceroni, F.; Corradi, M.; Gams, M.; Garbin, E.; Gattesco, N.; Krajewski, P.; et al. Glass fabric reinforced cementitious matrix: Tensile properties and bond performance on masonry substrate. *Compos. Part B Eng.* **2017**, *127*, 196–214. [CrossRef]
19. Garbin, E.; Panizza, M.; Valluzzi, M.R. Experimental Characterization of Glass and Carbon FRCMs for Masonry Retrofitting. *ACI Spec. Publ.* **2018**, *324*, 3.1–3.20.
20. CSLLPP. *Italian Standards: Guideline for the Identification, Qualification and Acceptance Control of Fibre Reinforced Cementitious Matrix (FRCM) Used for the Structural Consolidation of Existing Constructions*; CSLLPP: Rome, Italy, 2018.
21. De Felice, G.; Aiello, M.A.; Caggegi, C.; Ceroni, F.; De Santis, S.; Garbin, E.; Gattesco, N.; Hojdys, Ł.; Krajewski, P.; Kwiecień, A.; et al. Recommendation of RILEM Technical Committee 250-CSM: Test method for Textile Reinforced Mortar to substrate bond characterization. *Mater. Struct.* **2018**, *51*, 1–9. [CrossRef]
22. Ascione, L.; de Felice, G.; De Santis, S. A qualification method for externally bonded Fibre Reinforced Cementitious Matrix (FRCM) strengthening systems. *Compos. Part B Eng.* **2015**, *78*, 497–506. [CrossRef]
23. De Santis, S.; Hadad, H.A.; De Caso y Basalo, F.; de Felice, G.; Nanni, A. Acceptance criteria for tensile characterization of fabric-reinforced cementitious matrix systems for concrete and masonry repair. *J. Compos. Constr.* **2018**, *22*, 04018048. [CrossRef]
24. Ekenel, M.; y Basalo, F.D.C.; Nanni, A. Acceptance criteria for concrete and masonry strengthening using fabric-reinforced cementitious matrix (FRCM) and steel reinforced grout (SRG) composites. *ACI Spec. Publ.* **2018**, *324*, 4.1–4.6.
25. *AC434:2013*; AC434-ICC-Evaluation Service: Acceptance Criteria for Masonry and Concrete Strengthening Using Fiber-Reinforced Cementitious Matrix (FRCM) Composite Systems. ICC Evaluation. Services, Inc.: Los Angeles, CA, USA, 2013.
26. Carozzi, F.G.; Arboleda, D.; Poggi, C.; Nanni, A. Direct shear bond tests of fabric-reinforced cementitious matrix materials. *J. Compos. Constr.* **2020**, *24*, 04019061. [CrossRef]
27. Bellini, A.; Aiello, M.A.; Bencardino, F.; de Carvalho Bello, C.B.; Castori, G.; Cecchi, A.; Ceroni, F.; Corradi, M.; D'Antino, T.; De Santis, S.; et al. Influence of different set-up parameters on the bond behavior of FRCM composites. *Constr. Build. Mater.* **2021**, *308*, 124964. [CrossRef]
28. Lignola, G.P.; Caggegi, C.; Ceroni, F.; De Santis, S.; Krajewski, P.; Lourenço, P.B.; Morganti, M.; Papanicolaou, C.C.; Pellegrino, C.; Prota, A.; et al. Performance assessment of basalt FRCM for retrofit applications on masonry. *Compos. Part B Eng.* **2017**, *128*, 1–18. [CrossRef]
29. De Santis, S.; Ceroni, F.; de Felice, G.; Fagone, M.; Ghiassi, B.; Kwiecień, A.; Lignola, G.P.; Morganti, M.; Santandrea, M.; Valluzzi, M.R.; et al. Round Robin Test on tensile and bond behaviour of Steel Reinforced Grout systems. *Compos. Part B Eng.* **2017**, *127*, 100–120. [CrossRef]
30. Accardi, M.; Cucchiara, C.; La Mendola, L. Bond behavior between CFRP strips and calcarenite stone. In Proceedings of the 6th International Conference on Fracture Mechanics of Concrete and Concrete Structures, Catania, Italy, 17–22 June 2007; pp. 17–22.
31. Oddo, M.C.; Minafò, G.; La Mendola, L. Experimental investigation on tensile and shear bond behaviour of Basalt-FRCM composites for strengthening calcarenite masonry elements. *Procedia Struct. Integr.* **2023**, *44*, 2294–2301. [CrossRef]
32. Bramato, G.; Leone, M.; Aiello, M.A. Bond behaviour of externally bonded BALSALT-FRCM system and calcareous stone. *Procedia Struct. Integr.* **2023**, *44*, 2302–2309. [CrossRef]
33. Minafò, G.; La Mendola, L. Experimental investigation on the effect of mortar grade on the compressive behaviour of FRCM confined masonry columns. *Compos. Part B Eng.* **2018**, *146*, 1–12. [CrossRef]
34. *UNI EN ISO 13934-1*; Determination of Tensile Strength of Textile Fabric with Universal Tensile Strength Test Method. International Organization for Standardization: Geneva, Switzerland, 2013.
35. *UNI EN 1015-11*; Methods of Test for Mortar for Masonry–Part 11: Determination of Flexural and Compressive Strength of Hardened Mortar. International Organization for Standardization: Geneva, Switzerland, 2001.
36. RILEM Technical Committee 232-TDT (Wolfgang Brameshuber). Recommendation of RILEM TC 232-TDT: Test methods and design of textile reinforced concrete: Uniaxial tensile test: Test method to determine the load bearing behavior of tensile specimens made of textile reinforced concrete. *Mater. Struct.* **2016**, *49*, 4923–4927. [CrossRef]
37. Grande, E.; Milani, G. Interface modeling approach for the study of the bond behavior of FRCM strengthening systems. *Compos. Part B Eng.* **2018**, *141*, 221–233. [CrossRef]
38. Nerilli, F.; Marfia, S.; Sacco, E. Nonlocal damage and interface modeling approach for the micro-scale analysis of FRCM. *Comput. Struct.* **2021**, *254*, 106582. [CrossRef]
39. De Felice, G.; D'Antino, T.; De Santis, S.; Meriggi, P.; Roscini, F. Lessons learned on the tensile and bond behavior of fabric reinforced cementitious matrix (FRCM) composites. *Front. Built Environ.* **2020**, *6*, 5. [CrossRef]
40. Calabrese, A.S.; D'Antino, T.; Colombi, P.; Poggi, C. Study of the influence of interface normal stresses on the bond behavior of FRCM composites using direct shear and modified beam tests. *Constr. Build. Mater.* **2020**, *262*, 120029. [CrossRef]